Ecological Engineering xxx (2016) xxx–xxx

Contents lists available at ScienceDirect

Ecological Engineering

journal homepage: www.elsevier.com/locate/ecoleng

Optimizing attraction flow for upstream fish passage at a hydropower dam employing 3D Detached-Eddy Simulation

David C. Gisen[a,*], Roman B. Weichert[a], John M. Nestler[b]

[a] Federal Waterways Engineering and Research Institute (BAW), Kußmaulstr. 17, 76187 Karlsruhe, Germany
[b] Fisheries & Environmental Services, 9320 Mt. Moriah Road, Edwards, MS 39066, USA

ARTICLE INFO

Article history:
Received 9 May 2016
Received in revised form
12 September 2016
Accepted 11 October 2016
Available online xxx

Keywords:
Fishway design
Fish migration
Tailrace
CFD
ADCP
OpenFOAM

ABSTRACT

Restoration of upstream fish passage requires construction of efficient fishways. Selection of attraction flow rates and entrance velocities is one of the fundamental research tasks on medium-sized German rivers as general recommendations are ambiguous.

We used a transient 3D Computational Fluid Dynamics model of a hydropower dam tailrace calibrated with Acoustic Doppler Current Profiler velocity data and Detached-Eddy Simulation turbulence modeling to produce seven flow fields. Hydraulic results were linked to fish performance by means of fish-size-speed relations (ethohydraulic scale).

Resulting attraction flow relationships agree well with literature recommendations if the competing flow is defined as the adjacent turbine flow. Further, we found that entrance velocity clearly determines the downstream influence of the attraction flow plume over the attraction flow rate if no rapid mixing is present.

1. Introduction

Compliance with the European Water Framework Directive requires restoration of river continuity by 2027 through construction of efficient fishways (Scholten et al., 2014). The fishways must enable all major migratory fish species to bypass dams that block their movements. In Germany, the medium-sized rivers Neckar (mean annual flow at mouth 145 m^3/s), Main (225 m^3/s), Moselle (328 m^3/s), and Weser (383 m^3/s) are extensively regulated. Fishways at most of their dams are either non-existent or non-operational, preventing migratory fish from accessing important upstream spawning and rearing habitats. Motivated by timely compliance with the requirements of the European Water Framework Directive, the Federal Waterways Engineering and Research Institute (BAW) and Federal Institute of Hydrology (BfG) embarked on an intensive program to develop guidelines that address critical questions associated with effective fishway designs and operations. The selection of attraction flow rate is one of the fundamental tasks.

The two major biological goals of fishway attraction design for upstream migrating fish are maximizing fish entry rates and minimizing search durations. Two design questions are crucial for meeting these goals: "Where should the fishway entrance be positioned?" and "How should the near-entrance flow field be specified?". Basic guidelines for entrance positions are well established (Clay, 1995; Larinier, 2002). In contrast, general attraction flow rate and entrance velocity recommendations are not scientifically founded and are, therefore, ambiguous (Katopodis, 2005). From a strictly biological view, the ideal attraction flow rate would equal the river discharge; however, water demands for other project purposes compete for water that could be used for fishway attraction (Williams et al., 2012) and overbuilt fishways are unnecessarily expensive to construct and operate. Therefore, fishway design requires that fishway size, location, and attraction flow properties be treated as an optimization problem.

We focused on the well-established hydraulic parameters of attraction flow rate Q_{attr} and velocity at the fishway entrance v_{entr} (mean and maximum values, cf. Fig. 7, Appendix A), but acknowledge that other variables can influence fish attraction including turbulence (Coutant, 1998), spatial and temporal derivatives of velocity (Goodwin et al., 2014), the release location of the attraction flow (Burnett et al., 2016), and noise, smell, temperature and oxygenation (Williams et al., 2012). For Q_{attr}, existing international guidelines differ widely in proposed percent ranges and associated reference values (Weichert et al., 2013). For example, US-American guidelines (NMFS, 2011) recommend between 5% and 10% of the design high flow (defined as "mean daily average streamflow that is exceeded 5% of the time" during migration periods) for salmonids on rivers with mean annual flow greater than about 28 m^3/s. Ger-

* Corresponding author.
E-mail addresses: david.gisen@baw.de (D.C. Gisen), roman.weichert@baw.de (R.B. Weichert), john.m.nestler@gmail.com (J.M. Nestler).

http://dx.doi.org/10.1016/j.ecoleng.2016.10.065

man (DWA, 2014) and British (EA, 2010) guidelines refer to Larinier (1992, 2002), who generally recommends "approximately 1–5% of the competing flow" during the migration period for "well-positioned entrances". Larinier (2008) specifies the percent range to 2–5% of the competing flow defined as "either the turbine discharge, the ecological flow or the spilling discharge at the dam". However, it is still left to the judgment of the designer to determine fixed values or operating limits within these ranges.

Only a few published investigations document detailed tests of alternative Q_{attr} at hydropower dams. Weichert et al. (2013) conducted hydraulic physical model investigations for the Lauffen dam (Neckar River). The authors proposed a Q_{attr} of 5% of the adjacent turbine flow during the design high flow with Q_{attr} decreasing in proportion to lowering tailrace water level as flows decrease. Mader et al. (2014) evaluated different percentage values for three sites using 2D numerical modeling and fish tagging, but found no correlation between attraction and flow rate. Other 3D numerical studies focused on positioning the fishway entrance based on overlaying fish tracks with hydraulic conditions (Andersson et al., 2012; Lindberg et al., 2013) or based solely on hydraulic conditions (Musall et al., 2008).

Our study aimed to use 3D transient CFD models to: (1) evaluate the benefits of a numerical modeling approach to design an optimal Q_{attr} and v_{entr} versus a literature recommended approach; (2) assess alternative Q_{attr} for their ability to create a continuous *migration corridor* as required by DWA (2014); (3) evaluate findings of Weichert et al. (2013) linking Q_{attr} to turbine flow and tailwater elevation; (4) explore the synergy between Q_{attr} and v_{entr} proposed by Larinier (2002) and Clay (1995). Meeting these objectives would be a step towards developing widely applicable guidelines for fishway entrance hydraulic conditions including refined estimates of Q_{attr} that balance environmental goals and economic realities.

2. Materials and methods

2.1. Study site

We conducted our studies at the Kochendorf Dam located in Bad Friedrichshall-Kochendorf, Germany, in the mid-reach (River-km 103.8) of the Neckar River. Kochendorf Dam is the 11th of 27 Neckar River barrages moving upstream from the confluence with the Rhine River. From the right to the left bank, the facility consists of double navigation locks, a 105 m-long navigation guide wall and a powerhouse (Fig. 1). Design hydraulic head of 8.0 m is used to power three vertical Kaplan turbines with a combined maximum discharge of $Q = 100\ m^3/s$ (mean annual flow = $88\ m^3/s$). The elbow-type draft tubes do not exhibit internal splitter walls common in larger draft tubes.

2.2. Boundary conditions

The proposed vertical-slot fishway has an operating flow of $Q_{Op} = 0.67\ m^3/s$ and head drops of 0.12 m at each internal weir. Fishway entrances are planned for both sides of the powerhouse and will be located immediately adjacent to the most outside draft tube outlets, per accepted guidance (Clay, 1995; Larinier, 2002; Williams et al., 2012; DWA, 2014). The dual locations minimize the *dead end effect* where fish following the bulk flow upstream are unable to locate the fishway entrance. Future plans will extend the existing draft tubes to the same longitudinal distance as the proposed fishway entrances (Fig. 2). Both entrance pools connecting the fishway bottom and the river bed have a bottom slope of 1:2 and point downstream (0° to the bulk flow) in compliance with DWA (2014). The right-most fishway pool will be connected to the left-bank fishway via a concrete channel (not shown) embedded in the draft tube

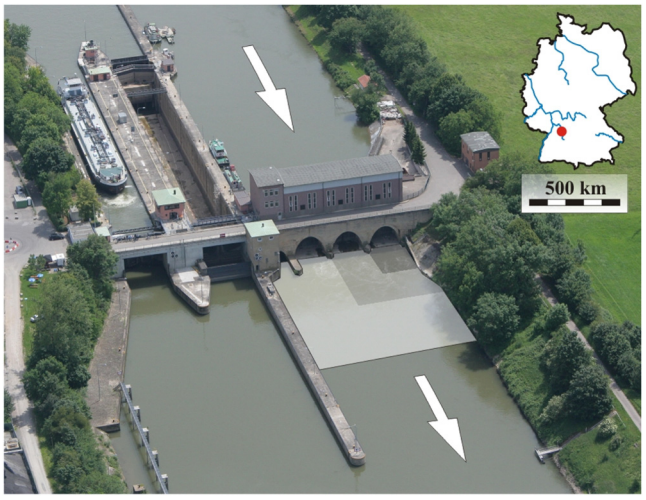

Fig. 1. Aerial view of Kochendorf double navigation lock (left), powerhouse (right), and tailrace model area (highlighted, darker areas show increasing mesh density). Insert shows site location (dot) at the Neckar River with respect to the German federal waterways (Courtesy Amt für Neckarausbau Heidelberg). Decimal degree coordinates: N 49.217348 E 9.207492.

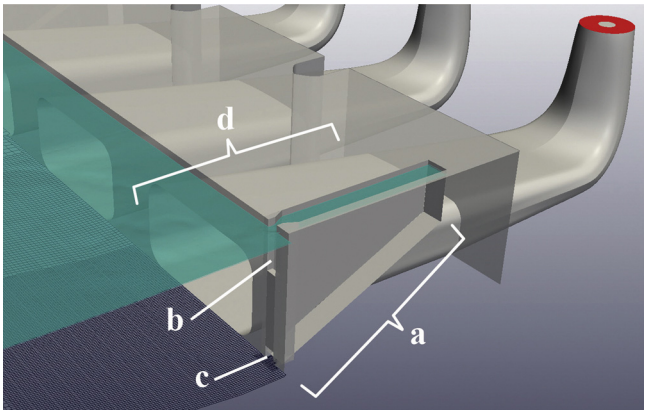

Fig. 2. (a) Left bank entrance pool of the projected fishway with (b) surface notch (0.5 m wide × 1.1 m high during low tailrace water level W_{30}) and (c) submerged orifice (0.5 m wide × 0.5 m high) adjacent to (d) the draft tube extensions. Flow from right (inlets) to left.

extensions. Auxiliary flow will be added through grates in the side walls of the fishway entrance pools.

German guidelines (DWA, 2014) specify the design and operation range for fishways from low (Q_{30}) to high flow conditions (Q_{330}) calculated from ranked, long term mean daily discharges and their corresponding tailrace water levels (W_{30} and W_{330}). Eliminating extreme dry or wet conditions from design considerations substantially simplifies fishway design and, therefore, reduces construction and operational costs. The high and low flow conditions for Kochendorf Dam (Table 3) serve as hydrological boundary conditions for two simulation scenarios.

Typically, fishway designers must consider three coupled entrance parameters: attraction flow rate Q_{attr}, mean entrance velocity $v_{design,entr}$, and water-level dependent cross-sectional area A. We varied Q_{attr} and $v_{design,entr}$ in four simulations for Q_{330} with full load of the powerhouse and three simulations for Q_{30}, where only the near-bank turbine was operational (Figs. 5 and 6 and Table 3). For the first run at Q_{330}, we selected $Q_{attr} = 5.1\%\ (1.70\ m^3/s)$ and $v_{design,entr}$ equal to the design velocity in the fishway (1.5 m/s) closely matching recommendations from Weichert et al. (2013). Thus, we determined A and fixed it for all subsequent analyses after making sure width and height of the openings (Fig. 2) matched

Please cite this article in press as: Gisen, D.C., et al., Optimizing attraction flow for upstream fish passage at a hydropower dam employing 3D Detached-Eddy Simulation. Ecol. Eng. (2016), http://dx.doi.org/10.1016/j.ecoleng.2016.10.065

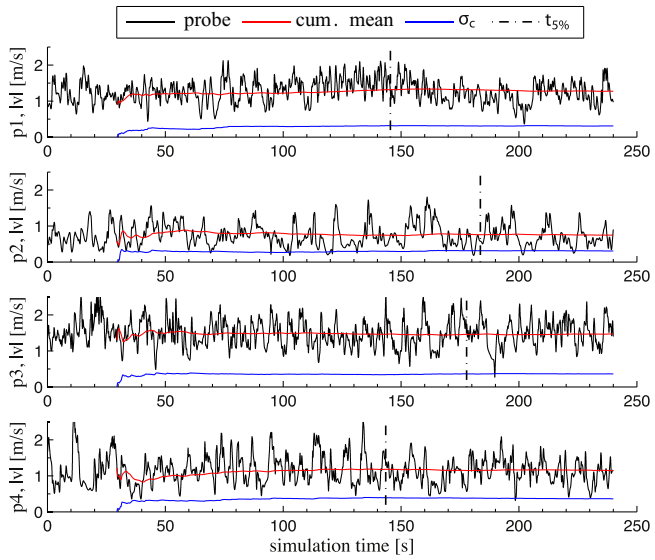

Fig. 3. Velocity magnitude $|v|$ (m/s), cumulated mean value and cumulated standard deviation σ_c of $|v|$ over time at four probe points in a representative simulation. 5%-criterion is reached between $t_{5\%}$ = 143 s at probe *p4* and $t_{5\%}$ = 184 s at probe *p2*.

requirements for all 39 target species including schooling fish like allis shad (*Alosa alosa*). For the first run at Q_{30}, we selected $v_{design,entr}$ = 1.5 m/s as well. *A*, and therefore Q_{attr}, were smaller due to the reduced water level.

2.3. ADCP field study

Water velocity magnitudes and directions in proximity to the powerhouse were measured using an Acoustic Doppler Current Profiler (ADCP) with four echo-beams (Fig. 4a, b). ADCP measured velocity profiles collected from a moving vessel with usual data density (e.g. 4 transects, McElroy et al., 2012) might not be sufficiently accurate (Muste et al., 2004a) for model calibration in highly turbulent areas like a tailrace because the assumption of horizontally homogenous flow is clearly violated (Sokoray-Varga et al., 2011). We used time-averaging to obtain data representative for the flow field and fixed vessel measurements to ensure spatial accuracy and high data density (Muste et al., 2004b). The ADCP probe was mounted below a trimaran that tracked along a steel cable stretched across the tailrace. We sampled each depth profile for 10 min in accordance with earlier experiences (Sokoray-Varga et al., 2011; Andersson et al., 2012) to achieve statistical stationarity of the data. We obtained an effective sampling frequency of approximately 2.5–3.5 Hz to average between 1500 and 2100 pings per profile.

2.4. Numerical model

We used the transient, fully 3D solver *interFoam* obtained from the open source toolbox OpenFOAM® (Weller et al., 1998) 2.1.0. *interFoam* discretizes the incompressible Navier-Stokes equations using the *Finite Volume Method* and solves the resulting equation system. The free surface is captured employing the *Volume of Fluid* method.

Flow patterns within bent draft tubes (without tailrace connection) have been simulated in detail in numerous studies with various codes including OpenFOAM (e.g. Cervantes et al., 2005; Page et al., 2010). Hydropower flow patterns in tailraces (without or with simplified, straight draft tubes) have been simulated using basic velocity inlet boundary conditions (Cook and Richmond, 2001; Musall et al., 2008). We combined the bent draft tubes and tailrace of our study site into one transient, free-surface simulation with a helical velocity inlet boundary condition to more accurately depict the interactions of the flows from the fishway entrances and the turbines.

We used *Delayed Detached-Eddy Simulation* (DDES; Spalart, 2009) as our turbulence model to more accurately simulate strong turbulent fluctuations typical for the case study area. DDES blends from conventional Reynolds-averaged turbulence modeling (RANS) in proximity of solid boundaries to Large Eddy Simulation (LES) in the bulk flow. This approach keeps mesh requirements moderate while providing superior turbulence representation in separated, high-Reynolds-number flows compared to standard RANS models (Spalart, 2009). Time step size ($\Delta t \approx 4.7$ ms) was dynamically controlled using a Courant-Friedrichs-Lewy (CFL) number of 0.3–0.4 in the main flow. Up to 60 processor cores were used per simulation on a high performance computer. Post-processing was done using MATLAB and ParaView software.

2.4.1. Computational mesh

We selected the near-bank draft tube and fishway entrance for detailed analysis because the most critical design questions were focused in this area. The model domain (cf. Fig. 1) was bounded laterally by the left bank and the lock guide wall. It extended downstream for 50 m to eliminate artificial boundary influences on the investigation area. We used a multibeam echo sounder to collect channel bathymetry data and created CAD drawings from *as built* plans that describe the concrete portion of the dam. The interior of the draft tubes was truncated as a plane just below the turbine runners. We imported the project geometry information into the mesh generator using a STL file format.

We created two hexahedron-dominant computational meshes with *snappyHexMesh*. At the near-bank draft tube and its wake, we refined edge lengths to 0.1 m based on a mesh dependency study which evaluated edge lengths of 0.2 m, 0.1 m, and 0.05 m. We placed five boundary layers contracting with a ratio of 1:2 at the near-bank draft tube walls to optimally fit the curved geometry. With increasing distance, we used coarser cells of 0.4 m and 0.8 m edge length, but kept 0.2 m at the water surface. The mesh used for calibration studies (without fishway entrance) consisted of 1.44 million cells. For scenario analysis, we incorporated the near-bank lowermost fishway pool and refined cells near the fishway entrance to a 0.05 m edge length to create a mesh containing 1.82 million cells.

2.4.2. Numerical boundary conditions

In 3D simulations, the influence of roughness on the solution is generally reduced compared to 1D or 2D simulations (Morvan et al., 2008). This is particularly true when flow pattern is dominated by the geometry, as in this case, allowing us to apply a smooth no-slip condition to the solid boundaries. For the downstream outlet, we applied a fixed stage condition. At the upstream draft tube inlets, the rotation of the turbine runners creates a helical vortex (i.e., a swirl) within the draft tube that produces flow asymmetry within and downstream of the draft tube. We applied radius-dependent turbine velocity vectors for u_t, v_t, and w_t as a custom boundary condition to qualitatively capture swirl effects (De Cachard et al., 2014). We calculated axial velocity from the flow rate divided by the inlet area as $u_t = Q_{turb}/A_t$. We computed the radius-dependent tangential velocity w_t using constant *swirl factor* s_t as $w_t(r) = r/R \cdot s_t \cdot u_t$. The quotient of actual distance from center r and shroud radius R increased linearly from *0* at the center to *1* at the outer edge, approaching the characteristics of data measured in a model draft tube (Cervantes et al., 2005). Seen from a bird's eye view, positive s_t resulted in a counter-clockwise swirl, and negative s_t resulted in a clockwise swirl. The radial velocity v_t was neglected and s_t was calibrated employing field data as described in Section 3.1.

Please cite this article in press as: Gisen, D.C., et al., Optimizing attraction flow for upstream fish passage at a hydropower dam employing 3D Detached-Eddy Simulation. Ecol. Eng. (2016), http://dx.doi.org/10.1016/j.ecoleng.2016.10.065

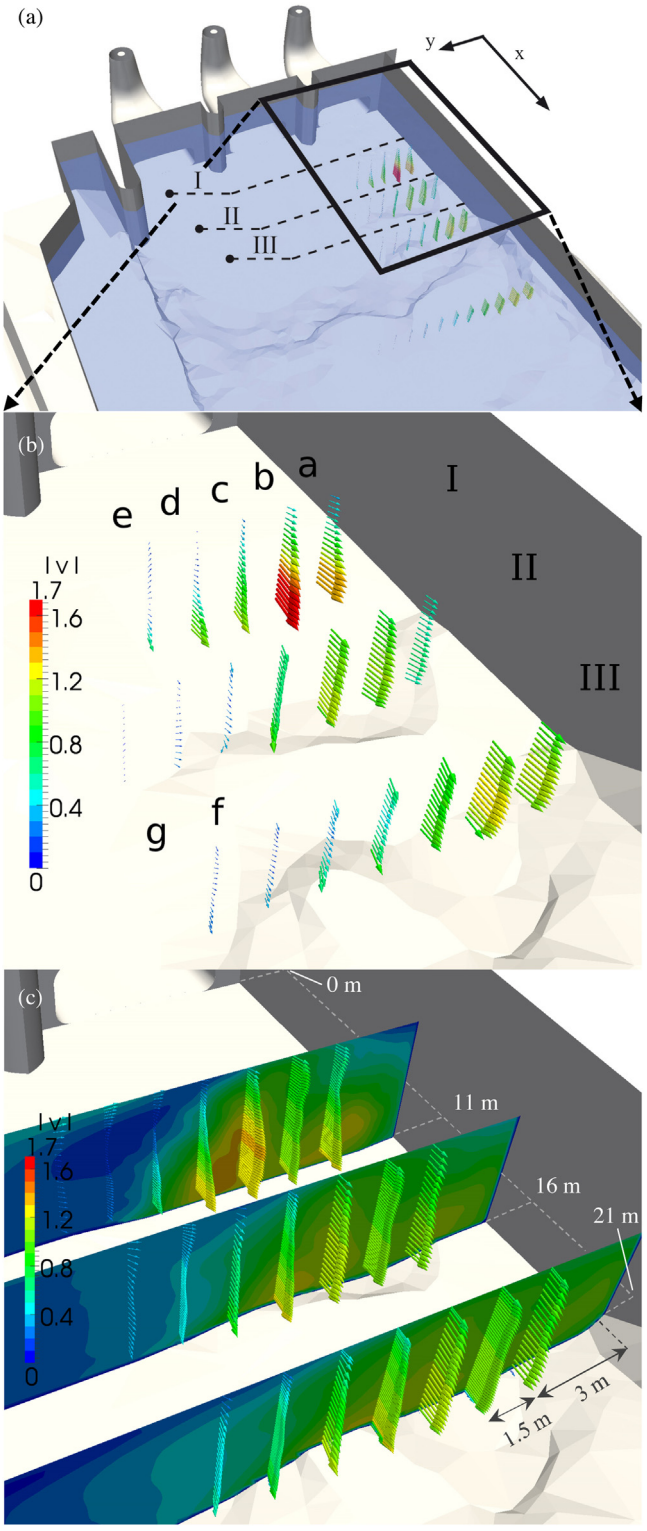

Fig. 4. (a) Positions of *transects I–III* in the field study. Mean discharge of the Neckar River on October 1 and 2, 2012, was about 28 m^3/s ($\sim Q_{30}$) and mean water depth was about $d = 5.51$ m ($W_{30} + 0.12$ m) at the draft tube outlet. Only the near-bank turbine was operational. Measurements closer to the powerhouse were not conducted because of partially strong water surface fluctuations in front of the draft tube outlet, which could have weakened the accuracy. (b) Resulting velocity vectors of the field study in *depth profiles a–g*, *transects I–III*. (c) Resulting time-averaged velocity magnitude $|v|$ (m/s) transects of the numerical study with swirl factor $s_t = +0.1$.

2.4.3. Determining averaging time

Our transient simulations required time-averaging for effective scenario analysis. We started an initial simulation from zero movement and obtained a visually steady averaged flow field after $t = 420$ s simulated time. This solution was used as the initial condition ($t_0 = 0$ s) for all subsequent simulations. To estimate an optimum time-averaging duration, we first created four virtual probes in the model located in a vertical plane 10 m downstream of the draft tube outlet. We output a time series record of velocity magnitude $|v|$ at each probe location ignoring the first 30 s (t_0 to t_{30}) to allow time for the modeled flow to stabilize. For times > t_{30} we calculated cumulative mean $|v|$ (sum of $|v|$ divided elapsed simulation time) and cumulative standard deviation σ_c (σ_c calculated over elapsed simulation time) at each subsequent time step. We set a criterion for averaging time, $t_{5\%}$, when the change in σ_c within a time span of 30 s became less than 5%. We chose $t_{5\%} = 150$ s for calibration conditions (Fig. 3) and $t_{5\%} = 210$ s for scenario simulations and averaged data between t_{30} and $t_{5\%}$.

2.5. Ethohydraulic scale and migration corridor

Hydraulic results must be linked to fish performance to assess performance of alternative fishway designs and operations. We used rules-of-thumb for swimming speed (DWA, 2014) applied to fish-size-class ranges (Table 1) to define an *ethohydraulic scale*. Using this scale, we transformed the numerical data into heat maps (Section 3.2 and 3.3) based on the *ethohydraulic color scheme* of Adam and Lehmann (2011). We follow the conventions of Beamish (1978) for naming categories of fish swimming performance although other conventions are common. We present results for total length, $TL = 0.4$ m, because it applies to mature individuals of fish species common in the Neckar River like nase (*Chondrostoma nasus*) and barbel (*Barbus barbus*). For brevity, we omit our results for the smallest of the 39 target species with $TL = 0.15$ m because our conclusions were not affected.

We used the concept of the continuous *migration corridor* (DWA, 2014; Kampke et al., 2014) for interpreting our results. We define the migration corridor in the tailwater as the coherent volume of downstream-directed velocities (a) high enough to induce rheotactic orientation and (b) low enough to be passed by the target species. Fish migrating along the bank will encounter the hydraulic signature of the fishway and follow it to the fishway entrance. Fish migrating mid-channel will encounter the fishway signature as they search laterally for a way around the dam. To support these natural behaviors, we define the following goals for evaluating the attraction flow:

- extending the length of the near-bank migration corridor into the fishway.
- eliminating dead-water zones near the bank to prevent disorientation.
- extending mid-channel migration corridors into the fishway by establishing an early connection to the main flow released from the powerhouse.
- sufficient corridor width and height to allow large fish and schools to move and navigate without leaving the plume.

3. Results

3.1. Calibration

An excellent opportunity to calibrate the swirl factor s_t (Section 2.4.2) was afforded by the presence of a high velocity jet extending downstream in line with the near-bank draft tube middle axis and with laterally decreasing velocity (Fig. 4b, profile *Ib*). Model dis-

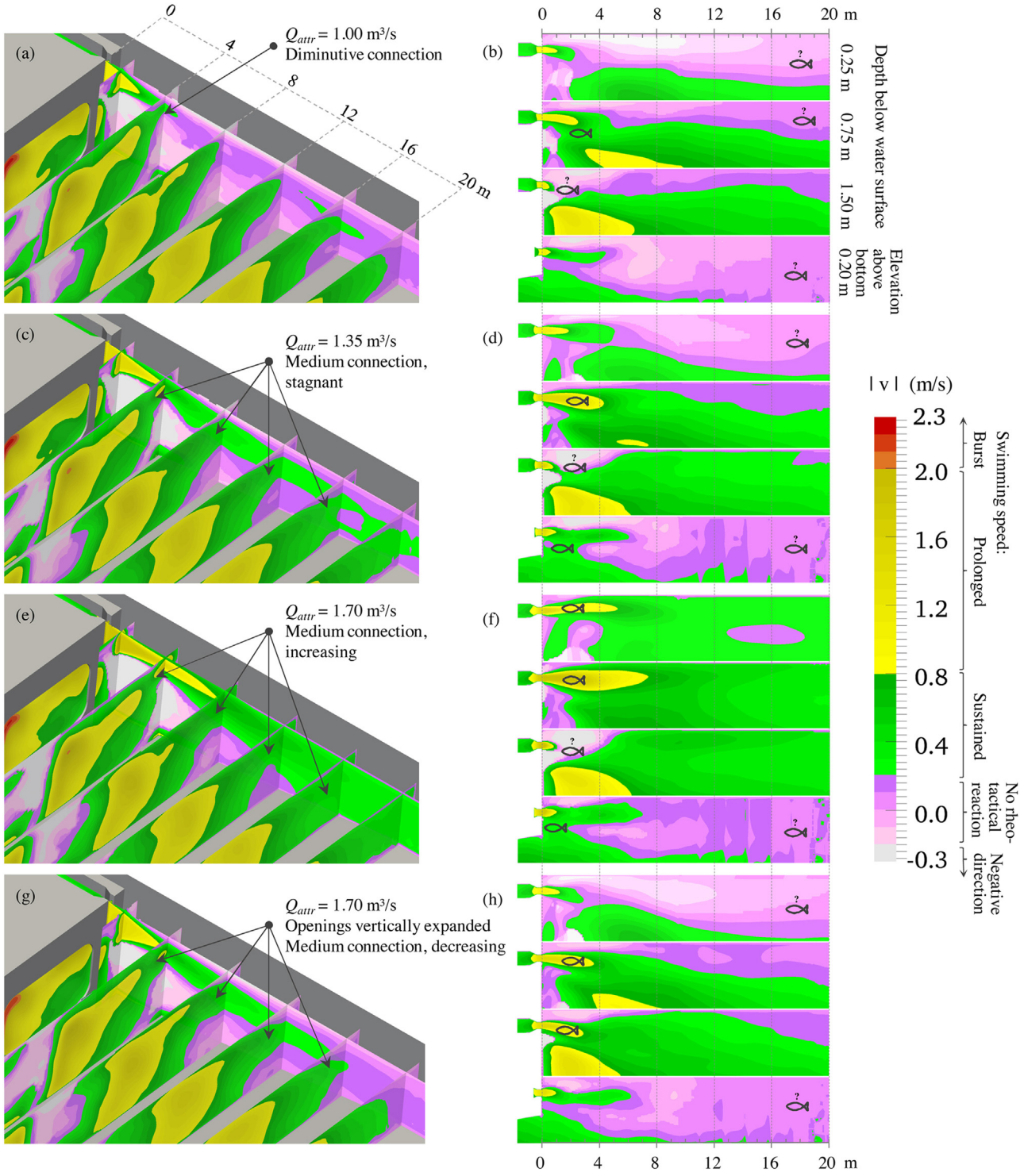

Fig. 5. High flow conditions: Transects and plan views of the tailrace for attraction flow rates (a, b) Q_{attr} = 1.70 m³/s, (c, d) 1.35 m³/s, (e, f) 1.00 m³/s, and (g, h) 1.70 m³/s with vertically expanded openings, respectively. Depicted is the time-averaged velocity magnitude $|v|$ (m/s). Positive and negative velocity signs were allocated according to the direction of the vectors' x components. Areas supporting attraction are marked with a fish symbol. Areas obstructing attraction are marked with a fish symbol and question mark.

charge and water level were set to match field study conditions. Time-averaged velocity vectors from the field study and model results were compared to identify an optimum value for s_t.

Generally, velocities were higher near the bottom and decreased with elevation in transect *I*, and were approximately constant over depth in transects *II* and *III*. We qualitatively evaluated characteristics of the jet in 16 calibration simulations using swirl factors in the range [−1, 1] and concluded, for draft tubes without splitter walls, that (a) swirl factors ranging from $s_t = \pm 0.05$ to $s_t = \pm 1$ generate single jets and (b) jet positions change only with the sign of the swirl factor and not with its magnitude. Based on visual similarity, we selected four simulations, *A–D*, for quantitative evaluation. For each simulation, we computed the *root mean square deviation* (RMSD) between simulation and field measurement by depth profile and averaged them for transects *I* and *III* (Table 2).

Please cite this article in press as: Gisen, D.C., et al., Optimizing attraction flow for upstream fish passage at a hydropower dam employing 3D Detached-Eddy Simulation. Ecol. Eng. (2016), http://dx.doi.org/10.1016/j.ecoleng.2016.10.065

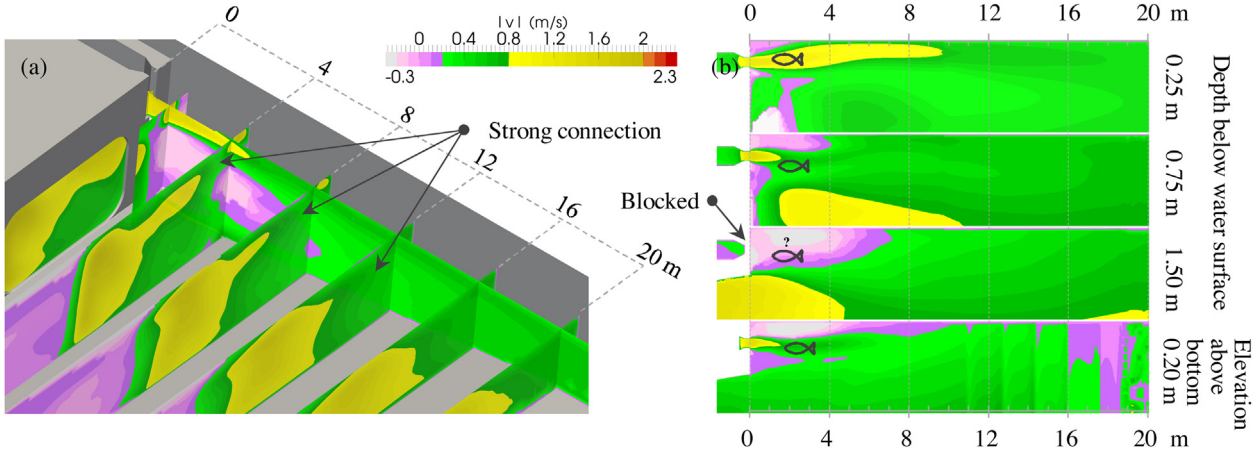

Fig. 6. Low flow conditions: (a) Transects and (b) plan views of the tailrace for medium attraction flow rate Q_{attr} = 1.00 m³/s. Results from the other two simulations were similar and are not depicted. See Fig. 5 for color and symbol explanations.

Table 1
Fish swimming speed classes and rules-of-thumb-ranges of fatigue times and flow velocities (DWA, 2014). *TL* is the total length.

Class name		Negative direction swimming speed	No rheotactical reaction	Sustained swimming speed[a]	Prolonged swimming speed[b]	Burst swimming speed[c]
Fatigue time		n/a	∞	> 200 min	200 min–20 s	20 s–1 s
Flow velocity	Range	< −0.2 m/s (non-salmonids) < −0.3 m/s (salmonids)	−0.2–0.2 m/s −0.3–0.3 m/s	up to 2 *TL*/s	2–5 *TL*/s	up to 20 *TL*/s ("small" fish) up to 10 *TL*/s (adult salmonids, cyprinids, percids)
	Applied to *TL* = 0.40 m	v ≤ −0.2 m/s	−0.2 < v ≤ 0.2 m/s	0.2 < v ≤ 0.8 m/s	0.8 < v ≤ 2.0 m/s	2.0 < v ≤ 4.0 m/s

[a] also "Cruising speed" (Goodwin et al., 2006; Clay, 1995; Bell, 1991).
[b] also "Sustained swimming speed" (Clay, 1995; Bell, 1991).
[c] also "Darting speed" (Clay, 1995; Bell, 1991) or "Sprint mode" (Castro-Santos, 2006).

Table 2
Jet features and computed *root mean square deviations* (RMSD) for selected field data transects and numerical simulations.

Identifier	Field	Sim. A	Sim. B	Sim. C	Sim. D
Swirl factor s_t	–	−0.1	0	+0.1	+0.5
$v_{jet,max}$ (m/s)	1.70	1.70	1.20	1.45	1.70
Approx. jet diameter (m)	2.0–2.5	3.0	two jets	2.0	2.0
Jet location	bottom	middle	bot–mid	bottom	mid–top
Avg. RMSD *I* (m/s)	–	0.337	0.330	0.334	0.553
Avg. RMSD *III* (m/s)	–	0.256	0.268	0.308	0.333

Table 3
Metrics of migration corridors from seven simulations (cf. Fig. 5). We defined the competing flow as the flow through the draft tube adjacent to the fishway entrance Q_{turb}. $v_{sim,entr,max}$ is the maximum simulated velocity in the entrance vicinity and $v_{design,entr}$ is the (mean) entrance velocity calculated by $v = Q/A$. Distances are measured from the fishway entrances and rounded to decimeters. *Prolonged distance* is the maximum extension of the isotach with v = 0.8 m/s and *Sustained distance* is the maximum extension of the isotach with v = 0.2 m/s. Infinity denotes that no extension limit could be identified. *mNN* is the vertical datum (*meters above Normalnull*).

	Hydrological conditions	Q_{330} = 100 m³/s			W_{330} = 143.64 mNN	Q_{30} = 29.9 m³/s		W_{30} = 142.97 mNN
	Q_{turb} (m³/s)	33.33				29.90		
	Identifier	low	medium	high	larger openings	low	medium	high
	Q_{attr} (m³/s)	1.00	1.35	1.70	1.70	0.80	1.00	1.20
	$v_{design,entr}$ (m/s)	0.9	1.2	1.5	1.2	1.0	1.3	1.5
	Q_{attr}/Q_{turb} (%)	3.0	4.1	5.1	5.1	2.7	3.3	4.0
Surface notch	$v_{sim,entr,max}$ (m/s)	1.1	1.5	1.9	1.5	1.5	1.7	1.9
	Prolonged distance (m)	2.8	4.5	7.7	4.7	6.7	9.8	19.8
	Sustained distance (m)	5.0	∞	∞	∞	∞	∞	∞
Submerged orifice	$v_{sim,entr,max}$ (m/s)	1.1	1.3	1.7	1.4	1.1	1.4	1.7
	Sustained distance (m)	5.0	6.0	7.2	6.3	5.5	∞	∞

Calibration simulation *D* was discarded because of high RMSD values and simulation *B* because of strong deviations in the jet form and velocity magnitude compared to field measurements. Simulations *A* and *C* rated equally well in terms of the above criteria, but we discarded simulation *A* because parts of its jet were positioned outside of the field data spatial domain. We selected the parameter

Please cite this article in press as: Gisen, D.C., et al., Optimizing attraction flow for upstream fish passage at a hydropower dam employing 3D Detached-Eddy Simulation. Ecol. Eng. (2016), http://dx.doi.org/10.1016/j.ecoleng.2016.10.065

set from simulation C (Fig. 4c) because of its good overall agreement with the field data and used it for scenario simulations.

3.2. Scenario simulations: high flow conditions

A continuous migration corridor towards the surface notch (cf. Fig. 2) was established in all three Q_{330} cases, but it was small with the low Q_{attr} (Fig. 5a, c and e and Table 3). The low and medium Q_{attr} both exhibited large dead-water zones at the surface and the bank (Fig. 5b and d). For the high Q_{attr}, the migration corridor extended downstream towards the bank and the main flow (Fig. 5f).

At the bottom orifice, a lateral migration corridor formed immediately downstream of the entrance for the medium and high Q_{attr}, but collapsed after a few meters (Fig. 5d and f). Large dead-water zones were present near the bottom in all cases. This weak expansion might be caused by the steeply rising bottom (~1:8) and by eddy creation from a large backflow zone in the wake of the baffle between the surface and submerged openings. To reduce this zone, a case with larger openings was investigated by extending the surface notch vertically by 0.5 m and the bottom orifice by 0.1 m for the high Q_{attr}. This reduced both mean and maximum entrance velocity compared to the high Q_{attr} (Fig. 5g and h and Table 3). The results were similar to the medium Q_{attr} and exhibited a large dead-water zone near the surface. We concluded the high Q_{attr} was optimal for Q_{330}.

We approached the assumption that both $v_{design,entr}$ and Q_{attr} are equally important for fish to locate the fishway entrance (Clay, 1995; Larinier, 2002) by comparing three of the previous simulations. We contrasted the downstream length of the influence of the fishway entrance plume of simulations in which Q_{attr} was held constant and $v_{design,entr}$ was decreased (case 1, "high" and "larger openings") with simulations in which $v_{design,entr}$ was held constant and Q_{attr} was decreased (case 2, "larger openings" and "medium"). We found that the maximum distance of prolonged swimming velocity decreased from 7.7 m to 4.7 m for case 1 (Fig. 5a, b, g and h and Table 3), but did not change for case 2 (4.7 m to 4.5 m, Fig. 5c, d, g and h). The Q_{attr} variation in case 2 only influenced the plume cross-section area close (< 5 m) to the entrances.

3.3. Scenario simulations: low flow conditions

The plumes for both the surface notch and submerged orifice for the Q_{30} high Q_{attr} expanded widely into longitudinal and lateral directions, creating continuous migration corridors. The submerged orifice plume exhibited a significantly larger expansion for Q_{30} than for Q_{330}. This caused the notch and submerged orifice plumes to converge about 7.4 m downstream of the two openings, a behavior not observed for Q_{330}. At the medium Q_{attr} (Fig. 6), the submerged orifice flow mixed with the turbine discharge plume, but nearly fell below the rheotactical threshold speed. We did not observe a mixing of the turbine discharge plume at the low Q_{attr}. We concluded that for Q_{30} the medium Q_{attr} with $v_{design,entr}$ = 1.3 m/s (instead of Q_{330} $v_{design,entr}$ = 1.5 m/s) were optimal design parameters.

4. Discussion

4.1. Attraction flow rate Q_{attr}

Generally, there are four approaches for design engineers to estimate the optimum attraction flow rate Q_{attr} by increasing effort and decreasing uncertainty: (a) general recommendations from the literature, (b) specific hydraulic model investigations, (c) coupled fish behavior and hydraulic model investigations, and (d) flexible construction supplemented with follow-up monitoring and assessment ("adaptive management"). We evaluate the performance of approach (a) versus approach (b), assuming that Q_{attr} percentages across multiple dams are comparable if entrance position, competing flow, and entrance configuration (Bunt, 2001) are similar. We treat other variables as random effects and neglect them during analysis (cf. Section 4.3).

We used the general recommendations (Q_{attr} = 2–5% of the competing flow) of Larinier (2002, 2008) as a basis, as the author shows a large number of citations (German, British, Austrian, and Swiss guidelines, see Weichert et al. (2013) for a comprehensive list). We speculate that they originate from expert knowledge, because explicit investigations are not cited. Therefore, their context is unavailable which may lead to arbitrary interpretation. For example, in Kochendorf, lack of supporting evidence allows design engineers applying Larinier's recommendations to choose between $Q_{attr} = 0.02 \cdot 29.9\ m^3/s = 0.6\ m^3/s$ (Q_{30}, one turbine "competing") and $Q_{attr} = 0.05 \cdot 100.0\ m^3/s = 5.0\ m^3/s$ (Q_{330}, all turbines "competing"). For clarity, we refine Larinier's (2008) definition of the competing flow for hydropower dams, the "competing turbine discharge", as the *adjacent* turbine discharge. This is supported by our results showing that the influence of distant turbines on the attraction flow plume is negligible. The other two options by Larinier (2008) for defining the competing flow ("ecological flow" and "spilling discharge") are not covered.

With these clarified application conditions, Larinier's maximum recommendation agrees very well with our high flow conditions findings for Q_{attr} (5.1%) as well as Weichert et al.'s (2013) result (5.3%). For low flow conditions, both investigations identified values larger than Larinier's minimum recommendation (3.3% and 3.9%, resp.). Weichert et al. associated hydraulic change to water level instead of discharge. This is important because stage and discharge can be decoupled due to backwater effects from a downstream dam. The matching model results confirm our comparability assumption stated above, since there is a strong similarity between Kochendorf Dam and Lauffen Dam (documented in Heinzelmann et al., 2013), upon which the Weichert et al. (2013) results are based.

Unfortunately, finding studies dealing with Q_{attr} changes in detail is difficult because, even in the well-investigated Columbia River system, "few studies have provided information that allows mechanistic evaluation of [...] modifications" (Naughton et al., 2007). Comparison is often hindered because differences in entrance positions, dam geometry, and migration corridor attributes confound the effects of Q_{attr}. In the following, we discuss studies of rivers considerably larger and smaller than the Neckar River to evaluate Larinier's recommendations.

The strongest methodological similarity to our study is found in Musall et al. (2008), who assessed $Q_{attr} = 3\ m^3/s$ (0.8% of approx. 355 m^3/s adjacent turbine flow) using a 3D numerical model. However, the entrance was placed in a low energy zone above the draft tubes and oriented perpendicular to the main flow direction. Therefore, we are not convinced that the attraction flow plume connects to the main flow for all flow conditions. Results from Andersson et al. (2012) and Lindberg et al. (2013) ($Q_{attr} = 10\ m^3/s$, 1.3% of 750 m^3/s total turbine flow) cannot be compared to our study because of the great water depth at their powerhouse outlets (40 m vs. 5.6 m in the present study); however, their results confirm our methods for velocity measurement (Section 2.3). It remains unclear if these recommended percentages are smaller than Larinier's (2008) recommendations mainly because of geometry differences or competing flow differences. The NMFS (2011) general recommendations (cf. Section 1) indicate that even a higher percentage was needed, but we cannot address their guidance because their basis is not documented. Still, we find it more likely that the recommended maximum value of Q_{attr} = 5% should be decreased instead of increased at turbine discharges orders of magnitude higher than in the Neckar River.

Please cite this article in press as: Gisen, D.C., et al., Optimizing attraction flow for upstream fish passage at a hydropower dam employing 3D Detached-Eddy Simulation. Ecol. Eng. (2016), http://dx.doi.org/10.1016/j.ecoleng.2016.10.065

Based on a field investigation at the Ager River (mean annual flow at site ~3.25 m^3/s), Mader et al. (2014) concluded that successful detection of the entrance is independent of the Q_{attr} percentage (0.5–15%). This seems to be confirmed by Mader et al. (1998) on a small channel (2–10 m^3/s discharge), even though one entrance was "incorrectly positioned" at a distance of 280 m to the weir. There are several possible reasons for their findings. First, we note that Mader et al. (2014) only reported the number of fish that used the fishway and did not estimate the number of fish in the tailwater that were attempting to migrate. Therefore, estimates of fishway efficiency could have been confounded by different numbers of fish in the vicinity of the fishway during conduct of their studies. Second, scale effects can be important when comparing passage results between small and large river systems. Fish are thought to sense hydraulic patterns in their immediate vicinity (Goodwin et al., 2014). Consequently, fish can sense a greater proportion of the hydraulic pattern in a smaller system than in a larger system. It is plausible that the properties of the attraction flow plume have limited influence on attraction in smaller rivers.

4.2. Attraction flow velocity

We conclude from the comparison of attraction flow plumes in Q_{330} scenarios (Section 3.2) that $v_{design,entr}$ clearly determines the downstream distance of hydraulic influence over Q_{attr}. A plume that extends further downstream will have a greater encounter surface area than a plume that does not extend as far downstream. We speculate that this characteristic reduces fish search durations. For Q_{30}, velocity influence is reduced because the plume mixes rapidly. We conclude that the local flow field determines the utility of Weichert et al.'s (2013) proposal to choose the entrance velocity equal to the design velocity in the fishway.

4.3. Methodological uncertainties

To compare and evaluate the different scenarios, we used time-averaged velocity fields. This approach is traditionally chosen in hydraulic analysis of alternative fishway designs (cf. references Section 4.1), although we acknowledge time-varying conditions could be important. However, biological field data that describe the response of fish to flow field features are summarized using time-averaged hydraulic conditions. Therefore, there are little data and few methods available to interpret the biological consequences of time-varying hydraulic information. We also acknowledge that any number of factors in addition to hydraulic pattern, be them biotic (e.g., reproductive state) or abiotic (e.g., magnetic fields), could affect fish response to fishway design (Katopodis, 2015). We treat velocity changes and any additional factors as random effects (i.e., disappearing influence in the long-term mean) and do not address them explicitly. Encouragement comes from the fact that our conclusions regarding swimming performance are conservative because the majority of modeled velocities at examined profiles exceeded field measured velocities. In the future, when the necessary biological data become available, it may be useful to consider time-varying hydraulic analysis for fishway design or to incorporate additional external factors or internal states of fish into the analysis.

Our use of the swirl factor for calibration yielded reasonable results with acceptable computational cost. We achieved higher calibration accuracy by using the custom inlet boundary conditions than by using a simple homogenous inlet boundary condition (cf. Andersson et al., 2012). We would have preferred availability of a second calibration dataset that included Q_{330} turbine operation conditions for validating the inlet boundary used in this study. However, we note that during the field study the operational near-bank turbine was close to full load (i.e., Q_{330}) and we modeled the full draft tubes with an advanced turbulence model for calibration. Therefore, we conclude that there is good scalability to Q_{330} with all three turbines.

Fishway entrance geometry and angle towards the main flow direction were consistent with the latest German guidelines (DWA, 2014). We did not investigate these parameters because we judged their value added to the analysis to be small. Further, we chose not to investigate additional scenarios between or higher than the presented Q_{attr}. The addition of more hydraulic scenarios must be accompanied by increased precision in the biological criteria if the scenarios are to be meaningfully interpreted. Detailed field studies better describing fish behavior in response to hydraulic pattern are planned in the future for the Kochendorf fishway to help reduce many of these uncertainties.

4.4. Ethohydraulic scale

We chose the ethohydraulic scale (Section 2.5) for visualizing and assessing hydraulic model results with respect to fish swimming performance. We did not apply individual-based model frameworks (Goodwin et al., 2014) or algebraic approaches (Puertas et al., 2012; Castro-Santos, 2006). Therefore, neither interspecific and intraspecific variation in swimming performance (Castro-Santos, 2006), water temperature (Beach, 1984), turbulence (Wilkes et al., 2013), nor complex swim behaviors could be considered. Nevertheless, we felt the ethohydraulic approach was adequate for our application because:

- it is based on guidelines accepted in Germany (DWA, 2014),
- it is conservative (i.e., under-estimates fish swimming speed) compared to the swim speed–fatigue time curve for shad from Castro-Santos (2006),
- it does not require biological calibration, keeping in mind that performance data for most of the 39 target species are lacking,
- it allows a fishway design to be assessed for a variety of species of the same and larger fish total length *TL* (if they agree in minimum rheotactic reaction velocity).

However, the ethohydraulic scale approach can only assess passability of a fish through a hydraulic field; it cannot predict fatigue effects which need to be accounted for by the designer. A complete analysis must further include a scale for the weakest target species, which we omitted as it had no effect on our conclusions.

5. Conclusions

Using 3D unsteady numerical simulations of high-resolution (cell size ≈ 0.1 m, time step ≈ 4.7 ms), we were able to model the complex flow patterns in a hydropower dam tailrace with sufficient detail to evaluate alternative fishway attraction designs. Calibration of the turbine inlet boundary condition using field data was crucial because of the helical vortex created by the spinning runner blades. Time-averaged fixed-vessel ADCP measurements, inclusion of draft tubes into the model mesh and turbulence modeling with Delayed Detached-Eddy Simulation contributed to model quality by providing exceptional calibration detail and resolution for our hydraulic investigations. Heat maps summarizing fish swimming speeds based on total length (ethohydraulic scale concept) enabled relatively fast, intuitive, and easily interpretable evaluation of our 3D flow field results.

For high flow conditions (Q_{330}), our results confirmed Larinier's (2008) general recommendation that Q_{attr} should be up to 5% of the competing flow, which we redefined as the adjacent turbine flow rate. For low flow conditions (Q_{30}), we found a Q_{attr} exceeding Larinier's minimum recommendation which shows the need

Please cite this article in press as: Gisen, D.C., et al., Optimizing attraction flow for upstream fish passage at a hydropower dam employing 3D Detached-Eddy Simulation. Ecol. Eng. (2016), http://dx.doi.org/10.1016/j.ecoleng.2016.10.065

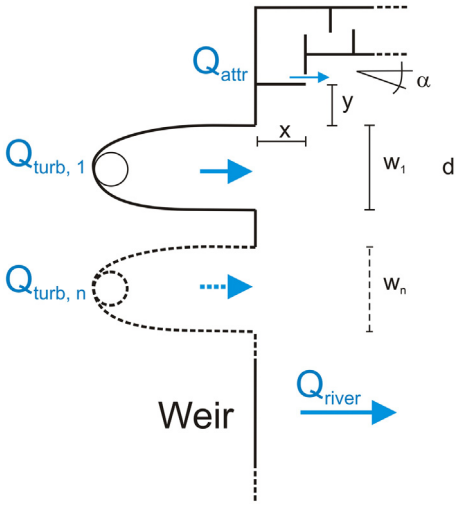

Fig. 7. Nomenclature of attraction flow parameters in a tailrace.

for accompanying application ranges. Further analysis showed that $v_{design,entr}$ clearly determined the length of the attraction flow plume over Q_{attr} when the plumes did not mix rapidly.

Undeniably, dimensioning of Q_{attr} using a percentage range is a major assumption, but, if valid, considerably simplifies fishway design. Our results show that such a general recommendation matched well to hydraulic model results under well-defined boundary conditions. We find it useful to interpret the percentage range in Larinier's recommendations as flow rates from minimum to maximum water levels. It is likely that this percentage range is different for different sized rivers, as our evaluation of studies indicated, even if they were not directly comparable to the present study. Therefore, we believe that further investigations are needed using a broader parameter base (parameter list suggestion in Appendix A) to reduce uncertainties and better define application ranges.

Acknowledgments

This article results from the joint research project "Ecological Continuity of Waterways" of the German Federal Institute of Hydrology (BfG) and the Federal Waterways Engineering and Research Institute (BAW) on behalf of the Federal Ministry of Transport and Digital Infrastructure. We gratefully thank two anonymous reviewers for providing insightful suggestions that improved the manuscript. Legal note: OPENFOAM® is a registered trademark of OpenCFD Limited.

Appendix A. Tailrace parameters

Parameter	Sign	Mader et al. (2014)	Present study	Heinzelmann et al. (2013)	Mader et al. (2014)	Musall et al. (2008)
River discharge(s) (ascending order)	Q_{river} [m³/s]	~3.25	29.9, 100	29.6, 166	135, 485	1420
Method applied	–	field study	3D numerical	lab model	2D numerical	3D numerical
Continuous migration corridor formed?	–	yes	yes	yes	no	?
Investigated attraction flow rate(s)	Q_{attr} [m³/s]	0.38, 0.42	1.0, 1.7	1.1, 2.1	4.9	3.0
Adjacent turbine discharge(s)	$Q_{turb,1}$ [m³/s]	3.25	29.9, 33.33	40	135	355
Attraction flow percentage of $Q_{turb,1}$	% [–]	0.5, 15.0	3.3, 5.1	3.9, 5.3	3.6	0.8
Mean entrance velocity	$v_{design,entr}$ [m/s]	0.34	1.3, 1.5	1.5, 1.5	~1.0	~1.3
Number of turbines	n [–]	1	3	2	4	4
Turbine field width(s)	w_i [m]	?	9.9	8.5	15, 15, 15, 20	27
Streamwise distance draft tube-entrance	x [m]	~10	0	0	~125	−10
Spanwise distance entrance-shore line	y [m]	?	0	0	2.5	0
Water depth(s) at entrance	d [m]	?	4.97, 5.64	3.98, 5.00	?	1.3
Entrance angle to main flow	α [°]	45	0	0	40	90
Grid resolution, if any	Δ [m]	–	0.1–0.8	–	?	0.25–4.0

Missing values were missing in the articles.

Appendix B. Supplementary data

Supplementary data associated with this article can be found, in the online version, at http://dx.doi.org/10.1016/j.ecoleng.2016.10.065.

References

Adam, B., Lehmann, B., 2011. Ethohydraulik: Grundlagen, Methoden und Erkenntnisse (Ethohydraulics: Basics, Methods, and Insights), 1st ed. Springer Verlag, Berlin/Heidelberg.
Andersson, A.G., Lindberg, D.-E., Lindmark, E.M., Leonardsson, K., Andreasson, P., Lundqvist, H., Lundström, T.S., 2012. A Study of the Location of the Entrance of a Fishway in a Regulated River with CFD and ADCP. Model. Simulat. Eng. 2012, 12 (Article ID 327929).
Beach, M.H., 1984. Fish pass design. In: Fisheries Research Technical Report 78. Min. Agric. Fish. Food, Lowestoft, England.
Beamish, F.W.H., 1978. Swimming capacity. In: Hoar, W.S., Randall, D.J. (Eds.), Fish Physiology, Vol. VII: Locomotion. Academic Press, London, pp. 101–187.
Bell, M.C., 1991. Fisheries Handbook of Engineering Requirements and Biological Criteria, 3rd ed. U.S. Army Corpy of Engineers, Portland, OR.
Bunt, C.M., 2001. Fishway entrance modifications enhance fish attraction. Fish. Manag. Ecol. 8 (2), 95–105, http://dx.doi.org/10.1046/j.1365-2400.2001.00238.x.
Burnett, N.J., Hinch, S.G., Bett, N.N., Braun, D.C., Casselman, M.T., Cooke, S.J., Gelchu, A., Lingard, S., Middleton, C.T., Minke-Martin, V., White, C.F.H., 2016. Reducing carryover effects on the migration and spawning success of sockeye salmon through a management experiment of dam flows. River Res. Appl., http://dx.doi.org/10.1002/rra.3051.
Castro-Santos, T., 2006. Modeling the effect of varying swim speeds on fish passage through velocity barriers. Trans. Am. Fish. Soc. 135, 1230–1237.
Cervantes, M.J., Engström, T.F., Gustavsson, L.H., 2005. Proc. third IAHR/ERCOFTAC Workshop on draft tube flows. In: Research Report No. 2005:20. Luleå University of Technology, Luleå, Sweden.
Clay, C.H., 1995. Design of Fishways and Other Fish Facilities, 2nd ed. Lewis Publishers, Boca Raton.
Cook, C.B., Richmond, M.C., 2001. Simulation of tailrace hydrodynamics using Computational Fluid Dynamics models. PNNL-13467. Pacific Northwest National Laboratory, Richland, Washington.
Coutant, C.C., 1998. Turbulent attraction flows for juvenile salmonid passage at dams. In: Report ORNL/TM-13608. Oak Ridge National Laboratory, Oak Ridge, TN.
DWA (Deutsche Vereinigung für Wasserwirtschaft, Abwasser und Abfall e.V.), 2014. Merkblatt DWA-M 509. In: Fischaufstiegsanlagen und fischpassierbare Bauwerke (Technical bulletin for fishways). Self-published, Hennef.
De Cachard, M., Roux, S., Boisson, N., Baux, Y., 2014. Digital simulation & experimental models: the experience of the Sauveterre fish pass. In: Proc. SymHydro 2014 Hydraulic Modeling and Uncertainty, Sophia Antipolis.
EA (Environment Agency), 2010. Environment Agency Fish Pass Manual: Guidance Notes on the Legislation, Selection and Approval of Fish Passes in England and Wales. Ver. 2.2. Environment Agency, Bristol, UK.
Goodwin, R.A., Nestler, J.M., Anderson, J.J., Weber, L.J., Loucks, D.P., 2006. Forecasting 3-D fish movement behavior using a Eulerian-Lagrangian-agent method (ELAM). Ecol. Model. 192, 197–223.
Goodwin, R.A., Politano, M., Garvin, J.W., Nestler, J.M., Hay, D., Anderson, J.J., Weber, L.J., Dimperio, E., Smith, D.L., Timko, M., 2014. Fish navigation of large dams emerges from their modulation of flow field experience. Proc. Natl. Acad. Sci. U. S. A. 111 (14), 5277–5282, http://dx.doi.org/10.1073/pnas.1311874111.
Heinzelmann, C., Weichert, R., Wassermann, S., 2013. Hydraulische Untersuchungen zum Bau einer Fischaufstiegsanlage in Lauffen am Neckar. (Hydraulic Investigations for the Construction of a Fishway in Lauffen at the

River Neckar). WasserWirtschaft 103 (1/2), 26–32.
Kampke, W., Weichert, R., Scholten, M., 2014. How to guide fish into a fishway? – Strategic aspects and investigations on attraction flow. In: Proc. 10th International Symposium on Ecohydraulics, Trondheim.
Katopodis, C., 2005. Developing a toolkit for fish passage, ecological flow management and fish habitat works. J. Hydraul. Res. 43 (5), 451–467.
Katopodis, C., 2015. A review of recent advances in ecohydraulics. In: E-proc. 36th IAHR World Congress, The Hague, 28 June–3 July.
Larinier, M., 1992. Implantation des passes à poissons. (Construction of fishways). Bull. Fr. Pêche Piscic. 326/327, 30–44.
Larinier, M., 2002. Location of fishways. Fishways: biological basis, design criteria and monitoring. In: Larinier, M., Travade, F., Porcher, J.P. (Eds.), Bull. Fr. Pêche Piscic. 364 (suppl), 39–53, ISBN 92-5-104665-4. Translation of Larinier (1992).
Larinier, M., 2008. Fish passage experience at small-scale hydro-electric power plants in France. Hydrobiologia 609 (5), 97–108.
Lindberg, D.-E., Leonardsson, K., Andersson, A.G., Lundström, T.S., Lundquist, H., 2013. Methods for locating the proper position of a planned fishway entrance near a hydropower tailrace. Limnologica 43, 339–347.
Mader, H., Unfer, G., Schmutz, S., 1998. The effectiveness of nature-like bypass channels in a lowland river, the Marchfeldkanal. In: Jungwirth, M., Schmutz, S., Weiss, S. (Eds.), Fish Migration and Fish Bypasses. Fishing News Books. Blackwell Science, Oxford, pp. 384–402.
Mader, H., Kraml, J., Lebiedzinski, K., Käfer, S., Mayr, P., 2014. Modelling and monitoring results of fish migration into fishpasses vs. attraction flow. In: Proc. 10th International Symposium on Ecohydraulics, Trondheim.
McElroy, B., DeLonay, A., Jacobson, R., 2012. Optimum swimming pathways of fish spawning migrations in rivers. Ecology 93 (1), 29–34.
Morvan, H., Knight, D., Wright, N., Tang, X., Crossley, A., 2008. The concept of roughness in fluvial hydraulics and its formulation in 1D, 2D, and 3D numerical simulation models. J. Hydraul. Res. 46 (2), 191–208.
Musall, M., Oberle, P., Fust, A., Nestmann, F., 2008. 3-D-Strömungssimulation zur Bewertung der Leitströmung eines Umgehungsgerinnes am Hochrheinkraftwerk Ryburg-Schwörstadt (3D flow simulation to evaluate the attraction flow of a bypass flume at the hydropower plant Ryburg-Schwörstadt). Wasserwirtschaft 98 (1/2), 37–42.
Muste, M., Yu, K., Spasojevic, M., 2004a. Practical aspects of ADCP data use for quantification of mean river flow characteristics; Part I: moving-vessel measurements. Flow Meas. Instrum. 15, 1–16.
Muste, M., Yu, K., Pratt, T., Abraham, D., 2004b. Practical aspects of ADCP data use for quantification of mean river flow characteristics; Part II: fixed-vessel measurements. Flow Meas. Instrum. 15, 17–28.
NMFS (National Marine Fisheries Service), 2011. Anadromous Salmonid Passage Facility Design. NMFS, Northwest Region, Portland, OR.
Naughton, G.P., Caudill, C.C., Peery, C.A., Clabough, T.S., Jepson, M.A., Bjornn, T.C., Stuehrenberg, L.C., 2007. Experimental evaluation of fishway modifications on the passage behaviour of adult Chinook salmon and steelhead at Lower Granite Dam, Snake River, USA. River Res. Appl. 23 (1), 99–111, http://dx.doi.org/10.1002/rra.957.
Page, M., Beaudoin, M., Giroux, A.M., 2010. Steady-state capabilities for hydroturbines with OpenFOAM. IOP Conf. Ser.: Earth Environ. Sci. 12, 012076, http://dx.doi.org/10.1088/1755-1315/12/1/012076.
Puertas, J., Cea, L., Bermúdez, M., Pena, L., Rodríguez, Á., Rabuñal, J.R., Balairón, L., Lara, Á., Aramburu, E., 2012. Computer application for the analysis and design of vertical slot fishways in accordance with the requirements of the target species. Ecol. Eng. 48, 51–60.
Scholten, M., Schütz, C., Wassermann, S., Weichert, R., 2014. Improving ecological continuity in German waterways: research challenges of upstream migration and fishway design. In: Proc. 10th International Symposium on Ecohydraulics, Trondheim.
Sokoray-Varga, B., Weichert, R., Lehmann, B., 2011. Flow investigations for fish pass Lauffen/Neckar in field and laboratory. Dresdner Wasserbauliche Mitteilungen 45, 87–94.
Spalart, P.R., 2009. Detached-Eddy Simulation. Annu. Rev. Fluid Mech. 41, 181–202, http://dx.doi.org/10.1146/annurev.fluid.010908.165130.
Weichert, R., Kampke, W., Deutsch, L., Scholten, M., 2013. Zur Frage der Dotationswassermenge von Fischaufstiegsanlagen an großen Fließgewässern (Investigations regarding guiding flow at fishways on German waterways). Wasserwirtschaft 103 (1/2), 33–38.
Weller, H.G., Tabor, G., Jasak, H., Fureby, C., 1998. A tensorial approach to CFD using object orientated techniques. Comput. Phys. 12 (6), 620–631.
Wilkes, M.A., Maddock, I., Visser, F., Acreman, M.C., 2013. Incorporating hydrodynamics into ecohydraulics: the role of turbulence in the swimming performance and habitat selection of stream-dwelling fish. In: Maddock, I., Harby, A., Kemp, P.S., Wood, P. (Eds.), Ecohydraulics. An Integrated Approach. , 1st ed. John Wiley & Sons, Ltd., pp. 9–30.
Williams, J.G., Armstrong, G., Katopodis, C., Larinier, M., Travade, F., 2012. Thinking like a fish: a key ingredient for development of effective fish passage facilities at river obstructions. River Res. Appl. 28, 407–417.

Please cite this article in press as: Gisen, D.C., et al., Optimizing attraction flow for upstream fish passage at a hydropower dam employing 3D Detached-Eddy Simulation. Ecol. Eng. (2016), http://dx.doi.org/10.1016/j.ecoleng.2016.10.065